Supplementary Information

1. Powder X-ray Diffraction Measurements

Figure S1. Diffractogram with Rietveld fitting for compound **1**. Red, Experimental data of X-ray powder diffractometry of compound **1**; Blue, Diffractogram simulated from single crystal X-ray determination; Green, Rietveld fitting.

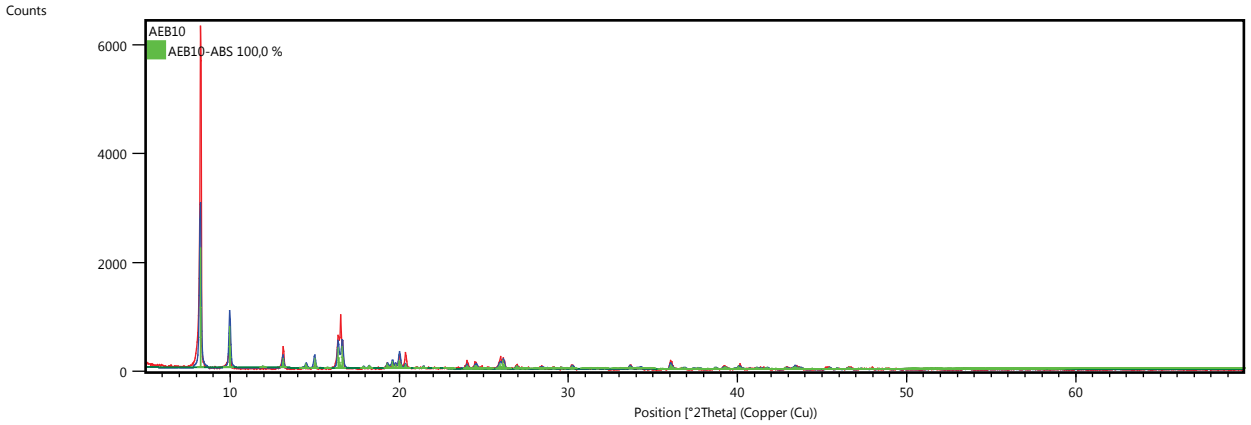

Figure S2. Diffractogram with Rietveld fitting for compound **2**. Red, Experimental data of X-ray powder diffractometry of compound **2**; Blue, Diffractogram simulated from single crystal X-ray determination; Green, Rietveld fitting.

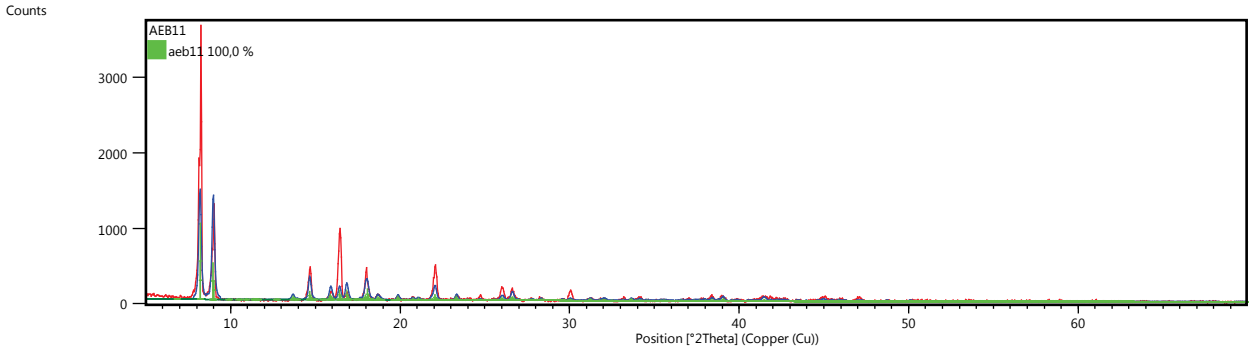

Figure S3. Diffractogram with Rietveld fitting for compound **3**. Red, Experimental data of X-ray powder diffractometry of compound **3**; Blue, Diffractogram simulated from single crystal X-ray determination; Green, Rietveld fitting.

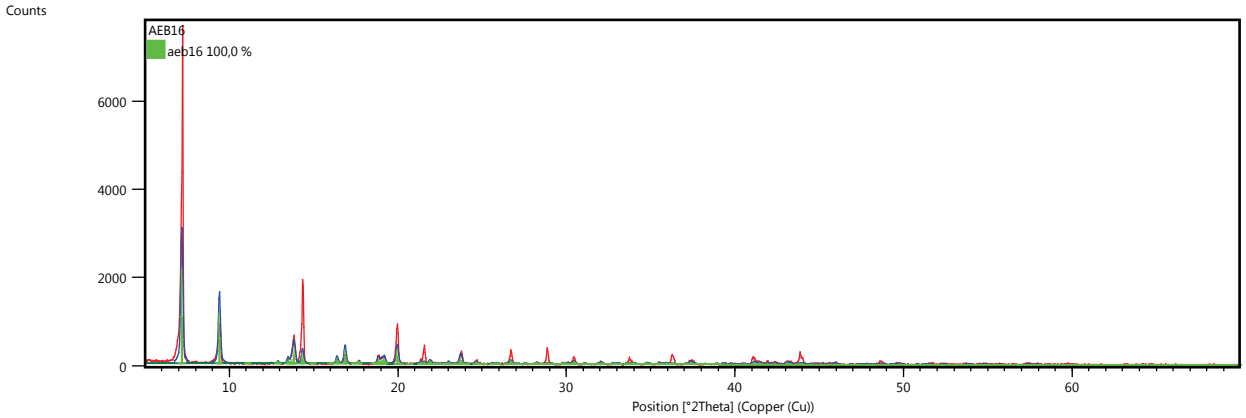

2. Infrared Spectra

Figure S4. IR spectrum of compound **1**.

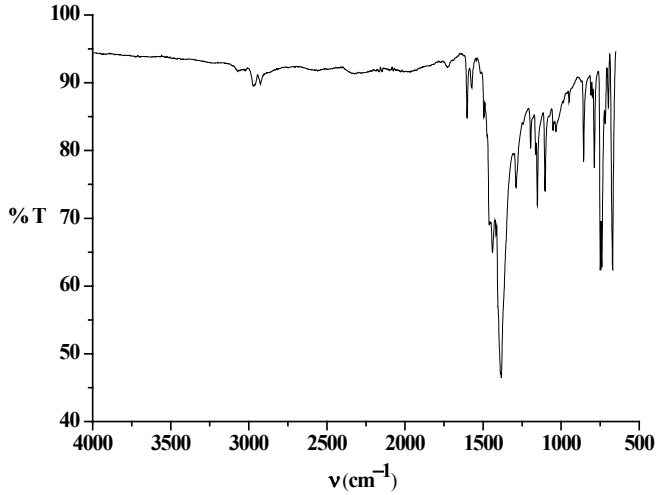

Figure S5. IR spectrum of compound **2**.

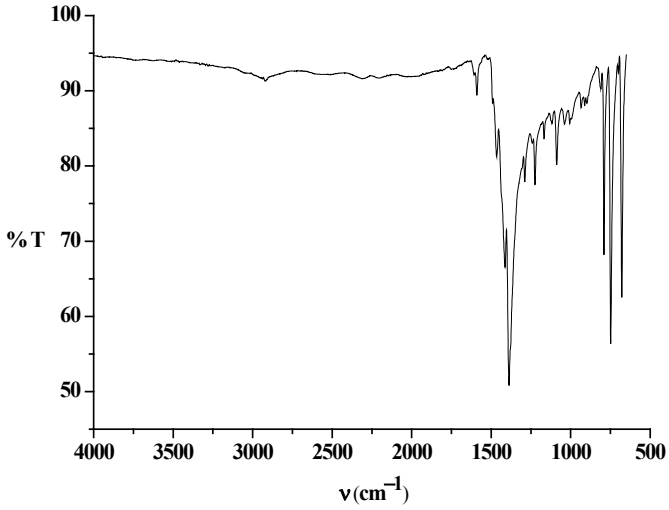

Figure S6. IR spectrum of compound **3**.

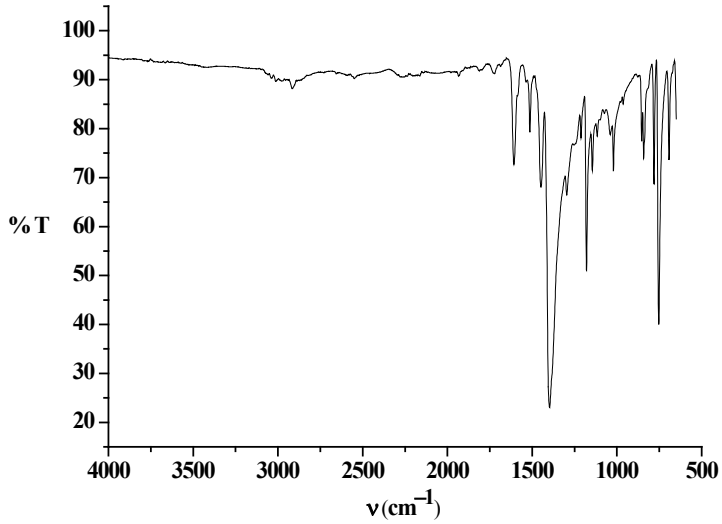

3. Electronic Spectra Data

Figure S7. Electronic spectra of compounds **1**–**3** measured by diffuse reflectance. The reflectance data were treated with Kubelka-Munk correction.

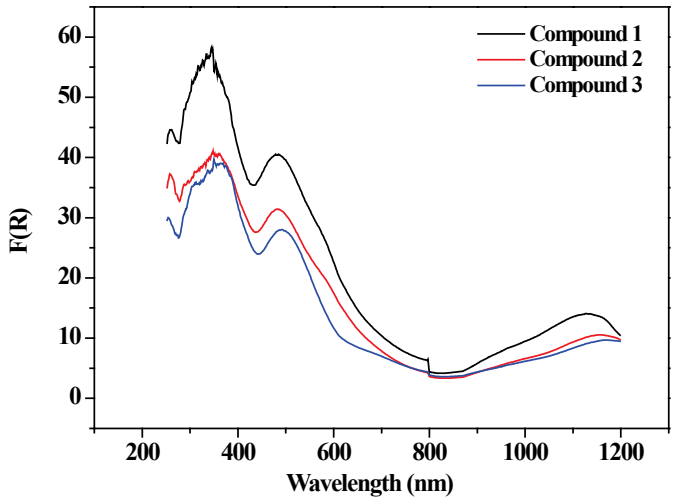

4. Magnetic Model

The model of Cukiernick *et al.* [31] takes into account the existence of a zero field splitting (D), a weak antiferromagnetic coupling (zJ') between the dimetallic units, a temperature independent paramagnetism (TIP) and a paramagnetic impurity (P) of a mononuclear complex of Ru(III) with $S = 1/2$. The zero field splitting effect on the susceptibility can be quantified by considering the Hamiltonian $H_D = S{\cdot}D{\cdot}S$. The perturbation of a weak antiferromagnetic coupling over the zero field splitting system can be considered by using the molecular field approximation. Thus, for an $S = 3/2$ spin system the magnetic susceptibility can be expressed as:

$$\chi' = \frac{\chi'_M}{1 - \chi'_M \left(\frac{2zJ'}{Ng^2\beta^2} \right)} \tag{1}$$

where χ_M' includes the TIP

$$\chi'_M = \chi_M + TIP \tag{2}$$

and χ_M considers the zero-field splitting in the parallel and perpendicular component as

$$\chi_M = \frac{\chi_{\parallel} + 2\chi_{\perp}}{3} \tag{3}$$

$$\chi_{\parallel} = \frac{Ng^2\beta^2}{kT} \left[\frac{1 + 9e^{-2D/kT}}{4\left(1 + e^{-2D/kT}\right)} \right] \tag{4}$$

$$\chi_{\perp} = \frac{Ng^2\beta^2}{kT}\left[\frac{4+\left(\frac{3kT}{D}\right)\left(1-e^{-2D/kT}\right)}{4\left(1+e^{-2D/kT}\right)}\right] \quad (5)$$

Finally, the consideration of the paramagnetic impurity (P) leads to the expression

$$\chi'_{mol} = (1-P)\chi' + P\frac{N\beta^2 g^2}{4kT} \quad (6)$$

Figure S8. Temperature dependence of the molar susceptibility χ_M (○) and $\mu_{eff.}$ (Δ) for complex **2**; solid lines are the product of a least-squares fit to the model indicated in the text.

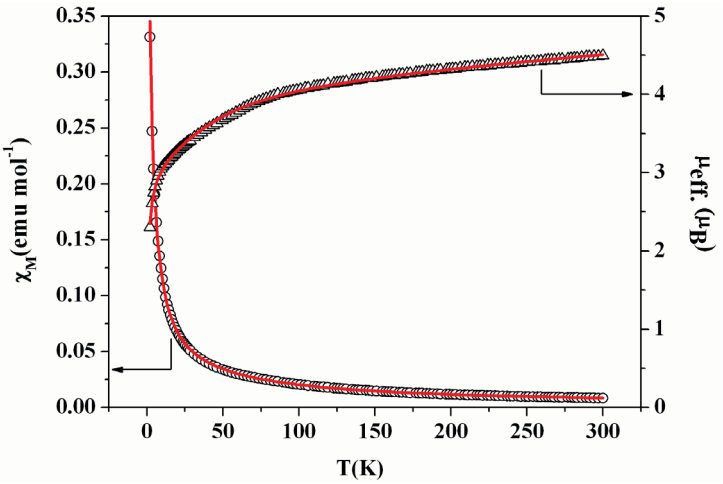

Figure S9. Temperature dependence of the molar susceptibility χ_M (○) and $\mu_{eff.}$ (Δ) for complex **3**; solid lines are the product of a least-squares fit to the model indicated in the text.